The Skin-Core Structure of Poly(acrylonitrile-itaconic acid) Precursor Fibers in Wet-Spinning

Heyi Ge,[1] Huashi Liu,[1] Juan Chen,[1] Chengguo Wang[2]

[1]*School of Material Science and Engineering, University of Jinan, Jinan 250022*
[2]*Carbon Fiber Engineering and Technology Research Center, School of Material Science and Engineering, Shandong University, Jinan 250061*

Received 30 July 2006; accepted 5 September 2007
DOI 10.1002/app.27286
Published online 18 January 2008 in Wiley InterScience (www.interscience.wiley.com).

ABSTRACT: The skin-core structure of poly(acrylonitrile-itaconic acid) [P(AN-IA)] precursor fibers in wet-spinning has been analyzed by the means of electron probe microanalyser (EPMA), scanning electron microscope (SEM), and transmission electron microscope. The numerical solution of Fick's second law equations for diffusion in the nascent fiber was obtained by using the Method of Lines. It has been found that [P(AN-IA)] precursor fiber composed of four parts had remarkable skin-core structure. The sheet-like skin, which was compact and homogeneous, had high crystallization and highly oriented structure. However, the core with low crystallization and some voids was loose, somewhat disorderly and unsystematic. Moreover, the precursor fiber had a pillar-like layered structure along the fiber axis. The average thickness of each layer increased gradually from the skin to the endothecium. Meanwhile, a structural model of PAN precursor fiber has been built. © 2008 Wiley Periodicals, Inc. J Appl Polym Sci 108: 947–952, 2008

Key words: P(AN-IA); wet-spinning; diffusion; skin-core structure; model

INTRODUCTION

Carbon fibers are becoming the key materials in aviation and composites due to their high performance. Now it has been widely convinced that the properties of carbon fibers are mainly determined by the microstructure of the precursor fibers because of the structural inheritance.[1–3] Acrylonitrile (AN) copolymer precursor fibers are the most successful and promising precursors for making high performance carbon fibers. The structure of acrylonitrile copolymer precursor fibers has substantial influence on the development of stabilized fibers and carbon fibers.[4,5] Therefore, the structure and the formation of acrylonitrile copolymer precursor fibers are of a great importance, which can facilitate the improvement of carbon fiber properties.

Although some literatures have reported the structure of acrylonitrile precursor fibers,[2-4,6] there are few studies on revealing the structure of acrylonitrile copolymer precursor fibers by transmission electron microscope (TEM) because it is pretty difficult to obtain some useful and integrated TEM images. In this study, the cross-sectional texture of poly(acrylonitrile-itaconic acid) [P(AN-IA)] nascent fiber and precursor fiber were investigated by electron probe microanalyser (EPMA) and scanning electron microscope (SEM), respectively. The numerical solution of Fick's second law equations for diffusion in the nascent fiber was obtained by using the Method of Lines (MOL) method. A more detailed analysis about the micromorphology of P(AN-IA) precursor fiber was carried out by TEM. Moreover, a structural model of PAN precursor fiber has been built.

EXPERIMENTAL

Wet Spinning

AN and IA were copolymerized in dimethylsulphoxide (DMSO) with azobisisobutyronitrile (AIBN) as radical initiator. The total concentration of monomers was controlled at 20 wt %. The ratio of AN/IA/AIBN is 98/2/0.8 (w/w/w). The reaction temperature was 60°C and the reaction time was about 8 h. The molecular weight (M_η) of P(AN-IA) was 1.44×10^5. Then the copolymer was purified and confected into a 20 wt % solution in DMSO.

The copolymer solution (dope) was vacuumized and filtered through a stainless steel mesh before spinning. Then the dope was extruded under pressure through a 1000-hole spinneret with 0.06-mm hole diameter and passed through three coagulation baths (70% DMSO, 30% DMSO, 10% DMSO) to get nascent fibers. Next, the nascent fibers were adequately

Correspondence to: C. Wang (wangchg@sdu.edu.cn).
Contract grant sponsors: National 863 Project, National Natural Science Commission.

Journal of Applied Polymer Science, Vol. 108, 947–952 (2008)

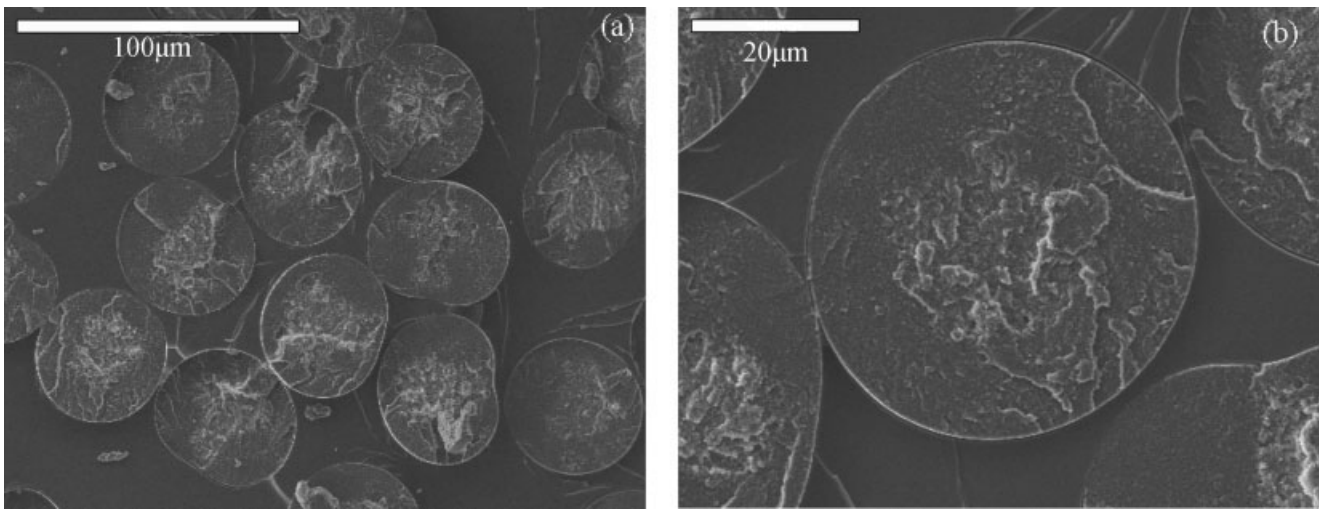

Figure 1 EPMA images of nascent fiber (a) the cross-sectional profile of nascent fiber, (b) the skin-core structure of nascent fiber.

washed with water and were drawn through three drawing processes including hot-water drawing, boiling-water drawing, and high-pressure-steam drawing. Finally, the filaments were finished, dried, and annealed to the precursor fibers.

EPMA

The nascent fibers were embedded in 191 no. unsaturated polyester resin and ruptured in liquid nitrogen. A JXA-8800R (Japan) EPMA operated at 20 kV was used to observe the cross-sectional microstructure.

Scanning electron microscopy (SEM)

A tow of precursor fibers was cut and embedded in E-44 epoxy resin. After solidification, the sample was polished. A HITACHI *S*-2500 (Japan) SEM operated at 20 kV was carried out on polished cross sections of precursor fibers to obtain SEM images.

TEM

The microstructure of precursor fibers was studied by a HITACHI H-800 (Japan) TEM operated at 150 kV. The samples of the fibers were ion-plasme etched in oxygen for 10–60 min. Then they were coated with a layer of gold (10–15-nm thick) in vacuum.

RESULTS AND DISCUSSION

Cross-sectional structure of nascent fiber

It is essential to study the nascent fiber structure as it exits from the coagulation baths to understand the actual influence on the structure of precursor fiber. Spinning dope was extruded to the coagulation bath under the pressure of the pump. There were mass transfer, heat conduction, and phase equilibrium movement between the streamlets of spinning dope and the surrounding medium, which led to the precipitation of P(AN-IA) and the formation of nascent fiber (gel fiber).[7] For the sake of mitigating the solidification, making the nascent fiber more uniform and reducing voids, three coagulation baths were introduced in this experiment. The cross-sectional profiles of nascent fiber are illustrated in Figure 1.

The streamlets of spinning dope was a true solution of P(AN-IA) copolymer, firstly. When the streamlets were extruded into the coagulation bath, there were two kinds of differential concentrations. Namely, the concentration of solvent (DMSO) in the streamlets was higher than that in the coagulation bath, and the concentration of nonsolvent (H_2O) in the streamlets was lower than that in the coagulation bath. Counterdiffusion of solvent and nonsolvent took place due to the differential concentrations, which was the fundamental process governing the fiber structure in wet spinning. The counterdiffusion occurred on the surface of the streamlets firstly and formed a layer of skin. The thin skin cumbered counterdiffusion process. As a result, the skin and the core had different densities, as shown in Figure 1(b). The skin-core structure in nascent fiber is obvious. The core region is loose with voids, whereas the outside region is more compact and dense.

Theoretical analysis of nascent fiber coagulation process

Fick's second law for diffusion in cylindrical coordinates is given by:

$$\frac{\partial c}{\partial t} = \frac{1}{r}\left\{\frac{\partial}{\partial r}\left(rD\frac{\partial c}{\partial r}\right)\right\} \quad (1)$$

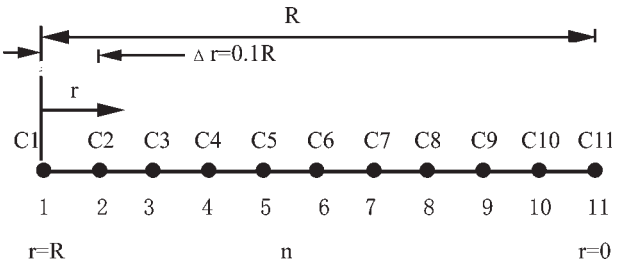

Figure 2 Diffusion in a one-dimensional radius direction.

where c represents solvent or nonsolvent concentration (mol/L), D is the diffusion coefficient (m^2/s), t is the time (s), and r is the distance from surface to center. The diffusion coefficient of solvent in this system has been calculated by Chen H.[8]

To solve the equation, initial and boundary conditions for a cylinder with radius R are given by:

$$\begin{aligned} &c = c_0 \quad \text{for } 0 \le r \le R \quad \text{at } t = 0 \\ &c = c_\infty \quad \text{for } t \ge 0 \quad \text{at } r = R \\ &\frac{\partial c}{\partial r} = 0 \quad \text{for } t \ge 0 \quad \text{at } r = 0 \end{aligned} \tag{2}$$

where c_0 represents the initial concentration of component in the filament and c_∞ represents the equilibrium concentration. The numerical solution of eq. (1) can be obtained using various methods such as finite difference method, finite element method, MOL, etc. MOL is a general technique for solving PDE by typically using finite difference relationships for the spatial derivatives and ordinary differential equations for the time derivative.

Considering the diffusion in the radial direction of filament, the finite difference of radius is shown in Figure 2. The radius is divided into 10 sections with 11 node points according to the initial and boundary conditions.

$$c_n = c_0 \quad \text{for } n = 2, 3, \ldots, 11 \text{ at } t = 0 \tag{3}$$

$$c_1 = c_\infty \quad \text{for } t \ge 0 \tag{4}$$

$$\frac{\partial c_{11}}{\partial r} = 0 \quad \text{for } t \ge 0 \tag{5}$$

For this problem with $N = 10$ sections of length $\Delta r = 0.1R = 3 \times 10^{-6}$ m, eq. (1) can be rewritten using a central difference formula for the second derivative as:

$$\frac{\partial c}{\partial t} = D\left(\frac{1}{(\Delta r)^2} + \frac{1}{r_n \Delta r}\right)c_{n+1} - D\left(\frac{2}{(\Delta r)^2} + \frac{1}{r_n \Delta r}\right)c_n + \frac{D}{(\Delta r)^2}c_{n-1} \quad \text{for } (2 \le n \le 10) \tag{6}$$

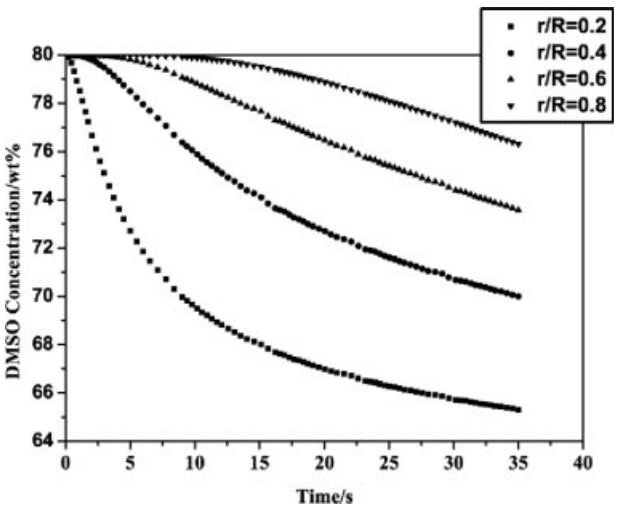

Figure 3 DMSO concentrations in different layers versus time.

The boundary condition represented by eq. (7) can be written using a second-order backward finite difference as:

$$\frac{\partial c_{11}}{\partial t} = \frac{3c_{11} - 4c_{10} + c_9}{2\Delta r} = 0 \tag{7}$$

Eqs. (4), (6), and (7) result in nine simultaneous ordinary differential equations and two explicit algebraic equations for the 11 concentrations at the various nodes. These equations can be solved with aid of Matlab.

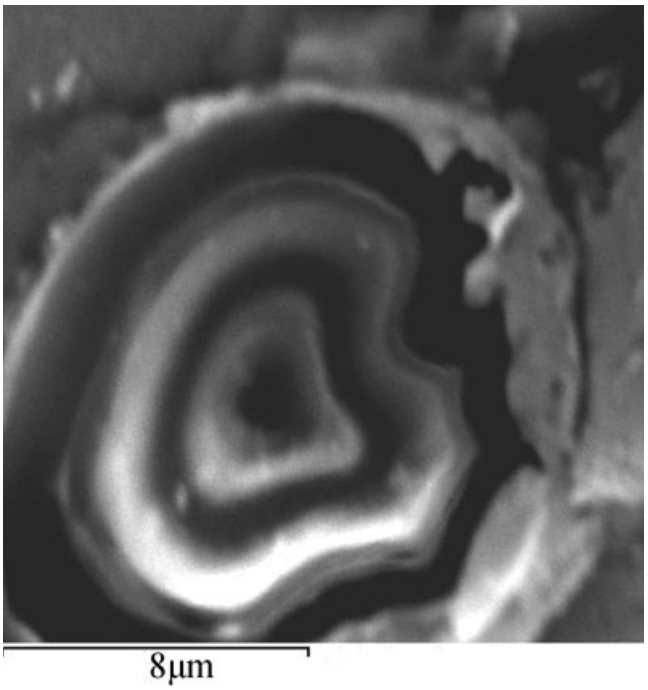

Figure 4 The cross-sectional SEM image of P(AN-IA) precursor fiber.

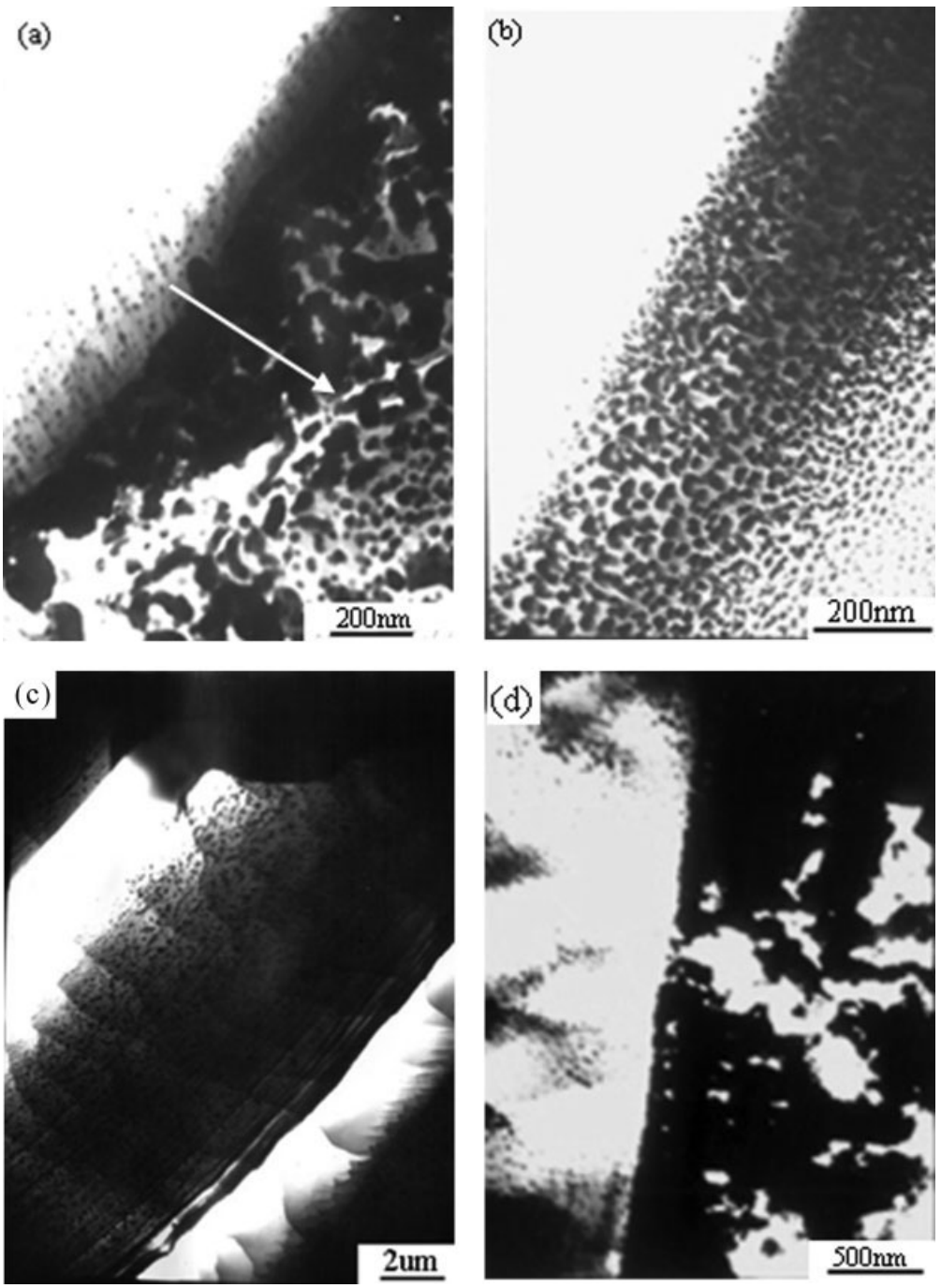

Figure 5 TEM images of P(AN-IA) precursor fiber (a) the multilayer structure of P(AN-IA) precursor fiber; (b) the skin; (c) the cortex; (d) the endothecium and the core.

Figure 3 shows the DMSO concentrations versus time in different layers. It can be seen that the DMSO concentration in outside layers (0.2R) decreases rapidly and it drops slowly in inner layers (0.8R). In outside layers, the outflow speed of DMSO is high initially due to the differential concentration, which leads to the rapid drop of DMSO concentration and results in polymer precipitation. Then a dense layer formed first. The coagulated dense layer will decrease the diffusion rate of inner layers. The different diffusion rates in various layers lead to polymer precipitated at various times, which may cause the nascent fiber has multilayer structure finally.

Cross-sectional structure of precursor fiber

The cross-sectional SEM photograph of P(AN-IA) precursor fiber is illustrated in Figure 4. It can be

clearly seen that P(AN-IA) precursor fiber has a skin-core morphology with multilayer concentric circles structure in the cross section, which is consistent with the foregoing theoretical analysis. The outermost white dense thin layer is the skin followed by the cortex, the endothecium and finally the core region. The interfaces are vivid. From the skin to the core, the thickness of each layer is about 0.2–0.3 μm, 2–3 μm, 2–3 μm, 6–7 μm, respectively. The structure was formed mainly due to the counterdiffusion motions in the coagulation process. With the concentration of the solvent (DMSO) in the filament incessantly decreasing, the concentrations of polymer, solvent, and nonsolvent would overcome the phase equilibrium conditions, which led to phase separation and the precipitation of the polymer.[9] The different rates of phase separation from the skin to the core caused the special structure from the nascent fiber to the precursor fiber.

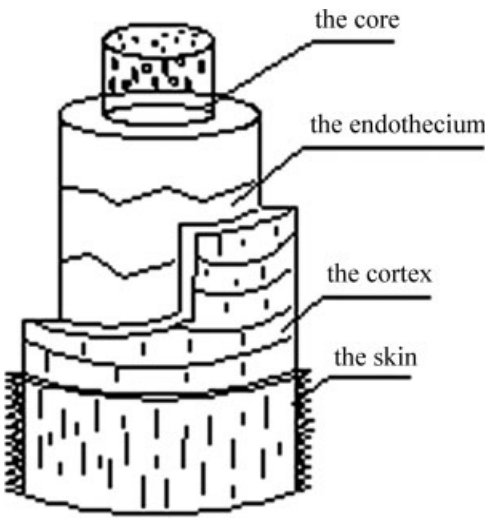

Figure 6 The structural model of PAN precursor fiber.

TEM investigation of precursor fiber

TEM images of skin-core microstructure of P(AN-IA) precursor fiber are shown in Figure 5. In Figure 5(a), the arrow, perpendicular to the fiber axis, points from the skin to the core. Figure 5(a) presents that the transverse microstructure of precursor fiber is a typical multilayer structure and clear interfaces exist between the layers, which accords with the image of SEM (Fig. 4). The skin composed of stacked layers has a sheet-like structure. The pretty thin sheets are almost perpendicular to the fiber axis. The structure of the sheets is dense and homogeneous. This might have been because phase separation firstly happened on the surface of the dope streamlets and formed a solid layer. Then, in the drawing process of coagulation bath, the solid skin endured tensile force mostly, which caused high crystallization and good orientation of molecular chains [Fig. 5(b)]. The size of each black crystallite in the skin was about 20–50 nm. Figure 5(c) illustrates that the cortex has a pillar-like layered structure, whose crystallites spread around evenly with good orientation along fiber axis. The thickness of each layer is about 1.5–2.0 μm. The endothecium also has a layered structure, but the delamination is not as clear as that of the cortex and each layer of the endothecium is thicker than that of the cortex [as shown on the left of Fig. 5(d)]. The core with some amorphous areas and voids was loose, somewhat disorderly and unsystematic [as shown on the right of Fig. 5(d)]. The endothecium and the core were initially viscous liquid in coagulation bath because their coagulation rate was slower than that of the cortex. The tensile force on them was lower, which might cause low crystallization and low orientation of crystallites.

The model of PAN precursor fiber

On the basis of the above experimental results, theoretical analysis and neglecting the interface effects, a structural model of PAN precursor fiber has been built (as shown in Fig. 6). The PAN precursor fiber, which can be considered four concentric cylinders, has the skin-core multilayer structure consisting of skin, cortex layer, endothecium layer, and core. The compact sheet-like skin with high crystallization and highly oriented crystallites is very thin and almost perpendicular to the fiber axis. The cortex, whose crystallites are well-dispersed with good orientation along fiber axis, is a pillar-like layered structure. The endothecium with blurry delamination is also composed of layers. The core texture is loose with voids. The endothecium and the core have low crystallization and low orientation of crystallites. Meanwhile, the precursor fiber has a pillar-like layered structure. The average thickness of each layer increases gradually from the skin to the endothecium. It is deduced that PAN crystallites are ordered into a liquid crystal-type array, giving in some cases a lamellar-like texture[10] and the increase of average thickness from the skin to the endothecium is due to the increase of amorphous (disordered) regions.

CONCLUSIONS

By systematic examination on the structures of P(AN-IA) nascent fiber and precursor fiber, using EPMA, SEM, and TEM, significant structural information has been obtained. P(AN-IA) precursor fiber in wet spinning had remarkable skin-core structure. The sheet-like skin, with high crystallization and

highly oriented crystallites, was compact and homogeneous. However, the core with low crystallization was loose, somewhat disorderly and unsystematic. Some defects, such as amorphous area and voids, were also observed in the cores. The formation of the skin-core morphology has been caused by the two diffusion motions in the coagulation baths of wet-spinning process. From these investigations, it can be concluded that controlling the microstructure of precursor fiber deliberately through optimizing coagulation bath technology is essential to reduce defects in the core, adjust the ratio of skin/core and obtain high properties of PAN precursor.

References

1. Kobets, L. P.; Deev I. S. Comp Sci Technol 1997, 57, 1571.
2. Chen, J. C.; Harrison, I. R. Carbon 2002, 40, 25.
3. Zhang, W. X.; Liu, J.; Wu, G. Carbon 2003, 41, 2805.
4. Jain, M. K.; Abhiraman, A. S. J Mater Sci 1987, 22, 278.
5. Huo, F.; Wang, F. Z. Carbon Fibers and Their Composites; Science Press: Beijing, China, 1995.
6. Liu, X. D.; Ruland, W. Macromolecules 1993, 26, 3030.
7. Bajaj, P.; Sreekumar, T. V.; Sen, K. J Appl Polym Sci 2002, 86, 773.
8. Chen, H.; Qu, R. J.; Liang, Y. J Appl Polym Sci 2005, 96, 1529.
9. Ziabicki, A. Fundamentals of Fiber Formation: The Science of Fiber Spinning and Drawing; Wiley: New York, 1976.
10. Warner S. B., Uhlmann D. R. J Mater Sci 1979, 14, 1893.